Turkish Journal of Chemistry

http://journals.tubitak.gov.tr/chem/

Research Article

Turk J Chem
(2014) 38: 454 – 469

doi:10.3906/kim-1304-88

Investigation of the adsorption kinetics of methylene blue onto cotton wastes

Bilal ACEMİOĞLU[1,*], Murat ERTAŞ[2], Mehmet Hakkı ALMA[3], Mustafa USTA[4]

[1]Department of Chemistry, Faculty of Science and Arts, Kilis 7 Aralık University, Kilis, Turkey
[2]Department of Forest Industrial Engineering, Faculty of Forestry, Bursa Technical University, Bursa, Turkey
[3]Department of Forest Industrial Engineering, Faculty of Forestry, Kahramanmaraş Sütçü İmam University, Kahramanmaraş, Turkey
[4]Department of Forest Industrial Engineering, Faculty of Forestry, Karadeniz Technical University, Trabzon, Turkey

Received: 03.05.2013 • **Accepted:** 04.11.2013 • **Published Online:** 14.04.2014 • **Printed:** 12.05.2014

Abstract: Cotton stalk (CS), cotton waste (CW), and cotton dust (CD), which are cotton wastes, were used as adsorbents to study the adsorption kinetics of methylene blue from aqueous solution. Kinetics of the batch adsorption experiment was investigated according to the pseudo-first order, the pseudo-second order, and the intraparticle diffusion models used commonly in the literature. The effects of the initial concentration, solution pH, and temperature on kinetic parameters (adsorption rate constant, initial adsorption rate, equilibrium adsorption capacity, etc.) were studied. The results showed that the adsorption process was well fitted to the pseudo-second order model for all adsorbents. The activation energy (E_a) of the adsorption process was determined by using the pseudo-second-order rate constants by means of Arrhenius' equation. The values of E_a were estimated as 7.05, 10.89, and 35.72 kJ mol^{-1} for CS, CW, and CD, respectively. From the results, it was understood that the adsorption process was controlled by an intraparticle diffusion mechanism as well as both an activated process and a physical adsorption process.

Key words: Cotton wastes, methylene blue, adsorption kinetics, activation energy

1. Introduction

The kinetic study of an adsorption process on a solid–liquid interface is a very important issue for a wide range of problems in pure and applied surface science. The explanation of the kinetics of an adsorption process provides information about the mechanism of adsorption. For example, the adsorption rate of a solute molecule (the residence time required for the completion of an adsorption reaction) may be estimated from kinetic analysis.[1] Moreover, the mechanism of interaction between a solid and a solute molecule may also be interpreted via kinetic studies. Many kinetic studies related to dye adsorption on low-cost adsorbent materials have been recorded in the literature. For example, Dogan and Alkan have studied the adsorption kinetics of methyl violet onto perlite.[2] Walker et al. have investigated the kinetics of the adsorption of a reactive dye onto dolomitic adsorbents.[3] Ho and McKay have evaluated the adsorption kinetics of acid blue 25 and basic blue 69 onto wood.[4] Kumar and Sivanesan have performed a study on the adsorption kinetics of safranin onto rice husk.[5] Ahmad and Kumar have studied the adsorption kinetics of amaranth dye onto alumina reinforced polystyrene.[6] Jovic-Jovicic et al. have evaluated the adsorption kinetics of acid orange 10 onto organobentonite as an adsorbent.[7] Senthilkumaar et al. have investigated the adsorption kinetics of direct blue and reactive blue by a lignocellulose-based waste

*Correspondence: acemioglu@kilis.edu.tr

biopolymer.[8] Hameed and El-Khaiary have studied the adsorption kinetics of methylene blue (MB) using broad bean peels.[9] Yao et al. have investigated the adsorption kinetics of MB by *Xanthoceras sorbifolia* seed coat (XSSC), a bioenergy forest waste.[10] Hameed et al. have also performed an equilibrium modeling and kinetic study on the adsorption of MB using coconut bunch waste.[11] In another work, we investigated the kinetics of a batch adsorption experiment of MB onto perlite.[12] In our previous study, we examined the adsorption of MB onto cotton stalk (CS), cotton waste (CW), and cotton dust (CD), which are cotton wastes.[13] However, a review of the literature reveals that no kinetics study on the adsorption of MB on CS, CW, and CD has been recorded, so far.

Therefore, the aim of the present study was to investigate the adsorption kinetics of MB from aqueous solution on CS, CW, and CD by batch adsorption technique in terms of the kinetic theories expressed below at different concentrations, pHs, and temperatures.

There are several kinetic models to clarify the mechanism of the adsorption process between a solute and an adsorbent. The equations of these kinetic models are given as follows.

a) The linear form of the pseudo-first-order kinetic model of Lagergren[14] can be expressed as

$$\log (q_1 - q_t) = log(q_1) - \frac{k_1}{2.303} t, \tag{1}$$

where k_1 is the rate constant of the pseudo-first-order kinetics ($\min^{-1}$), q_1 and q_t are the amounts of solute adsorbed on the surface of the adsorbent at equilibrium and any time (mg g^{-1}), and q_1 and k_1 are calculated from the intercept and the slope of plots of $\log (q_1 - q_t)$ vs. t, respectively. If the value of q_1 estimated from the intercept value does not equal the experimental data (q_e), the reaction is not likely to obey the pseudo-first-order kinetics model, even if this plot has a high correlation coefficient with the experimental data.

b) The linear form of the pseudo-second-order kinetic model of Ho[15,16] is given as

$$\frac{t}{q_t} = \frac{1}{k_2 q_2^2} + \frac{1}{q_2} t, \tag{2}$$

where k_2 is the rate constant of the pseudo-second-order kinetics (g mg^{-1} $\min^{-1}$), q_2 and q_t are the amounts of solute adsorbed on the surface of the adsorbent at equilibrium and any time (mg g^{-1}), and k_2 and q_2 are calculated from the intercept and the slope of plots of $\log\ t/q_t$ against t, respectively. Herein, $k_2 q_2^2$ is equal to h, and h indicates the initial rate of adsorption.

c) The equation of the intraparticle diffusion model of Weber and Morris can be expressed as[17]

$$q_t = k_i t^{1/2} + C, \tag{3}$$

where k_i is the intraparticle diffusion rate constant (mg g^{-1} $\min^{-1/2}$) and C is the intercept. This model reflects that pore diffusion occurs due to the porous nature of the adsorbent. The rate constant of intraparticle diffusion (k_i) can be estimated from the slope of the linear portion of the plot of the amount of solute adsorbed (q_t) against the square root of time ($t^{1/2}$).

2. Results and discussion

2.1. Equilibrium time

The adsorption of MB onto CS, CW, and CD was continued as a function of time until the amount of MB adsorbed became constant. This period was regarded as the equilibrium time for adsorption. The equilibrium

time was determined as nearly 90 min for all concentrations, pHs, and temperatures studied. The maximum amounts of MB adsorbed per unit mass of CS, CW, and CD at the equilibrium time (i.e. equilibrium adsorption capacities of CS, CW, and CD, q_e) increased with increasing initial dye concentration, pH, and temperature. The values of equilibrium adsorption capacity obtained under all the experimental conditions are given in Tables 1–9.

2.2. Effect of initial dye concentration on adsorption kinetics

For the adsorption of MB onto CS, CW, and CD, the effect of initial dye concentration was studied at 20 °C, pH 6.33, and 125 rpm as a function of contact time. When the initial MB concentration was increased from 25 to 100 mg L^{-1}, the values of equilibrium adsorption capacities of CS, CW, and CD increased from 1.96 to 5.95 mg g^{-1}, from 2.50 to 14.04 mg g^{-1}, and from 3.10 to 15.78 mg g^{-1}, respectively. A similar result was recorded for the removal of MB by green algae *Ulothrix* sp.[18]

2.2.1. The pseudo-first-order kinetics of MB adsorption on CS, CW, and CD for different initial dye concentrations

The pseudo-first-order kinetics of MB adsorption onto CS, CW, and CD were studied for different initial dye concentrations at 20 °C, pH 6.33, and 125 rpm.

For the adsorption of MB onto CS, the values of rate constants (k_1) estimated from the pseudo-first-order model decreased with an increase in the dye concentration, and they were determined as 5.30 × 10^{-2}, 4.0 × 10^{-2}, 4.40 × 10^{-2}, and 4.10 × 10^{-2} min^{-1} for initial dye concentrations of 25, 50, 75, and 100 mg L^{-1}, respectively. The correlation coefficients, r^2, obtained from the plots of *log* $(q_1 - q_t)$ vs. t had high values between 0.957 and 0.992; on the other hand, the values of equilibrium adsorption capacities (q_1) estimated from the intercept of the plots of *log* $(q_1 - q_t)$ vs. t were found to be 0.90, 1.15, 1.84, and 1.43 mg g^{-1} for initial dye concentrations of 25, 50, 75, and 100 mg L^{-1}, respectively. It appears that these theoretical values of q_1 are not in agreement with the experimental data (q_e) (see Table 1).

In the case of the adsorption of MB onto CW, the values of k_1 decreased with an increase in the initial dye concentration, and they were determined as 5.60 × 10^{-2}, 3.30 × 10^{-2}, 3.80 × 10^{-2}, and 3.6 × 10^{-2} min^{-1} for initial dye concentrations of 25, 50, 75, and 100 mg L^{-1}, respectively. The values of r^2 determined from the plots of *log* $(q_1 - q_t)$ vs. t were between 0.897 and 0.978. The values of q_1 were calculated as 0.56,

Table 1. Kinetic parameters for MB adsorption on CS at different initial dye concentrations.

C_0^a	q_e^b	q_2^c	k_2^d	h^e	r_2^{2f}	q_1^g	k_1^h	r_1^{2i}	k_i^j	C^k	r_i^{2l}
25	1.96	2.05	0.104	0.437	0.9997	0.90	0.053	0.979	0.109	1.045	0.869
50	3.59	3.68	0.083	1.122	0.9988	1.15	0.040	0.957	0.127	2.463	0.976
75	5.12	5.28	0.055	1.524	0.9995	1.84	0.044	0.992	0.212	3.304	0.931
100	5.95	6.06	0.074	2.713	0.9997	1.43	0.041	0.979	0.172	4.466	0.911

[a] Initial dye concentration (mg/L), [b] Equilibrium adsorption capacity obtained as experimental (mg/g), [c] Equilibrium adsorption capacity obtained from the pseudo-second-order equation (mg g^{-1}), [d] The rate constant of the pseudo-second-order reaction (g/mg min), [e] The initial adsorption rate from the pseudo-second-order kinetics (mg/g min), [f] Correlation coefficient from the pseudo-second-order equation, [g] Equilibrium adsorption capacity obtained from the pseudo-first-order equation (mg/g), [h] The rate constant of the pseudo-first-order reaction (1/min), [i] Correlation coefficient from the pseudo-first-order equation, [j] Intraparticle diffusion rate constant (mg/g $min^{1/2}$), [k] Intercept from the intraparticle diffusion equation, [l] Correlation coefficient from the intraparticle diffusion equation.

0.57, 1.19, and 1.87 mg g^{-1} for initial dye concentrations of 25, 50, 75, and 100 mg L^{-1}, respectively. The values of q_1 were not in agreement with the experimental data, q_e (see Table 2).

Table 2. Kinetic parameters for MB adsorption on CW at different initial dye concentrations.

C_0^a	q_e^b	q_2^c	k_2^d	h^e	r_2^{2f}	q_1^g	k_1^h	r_1^{2i}	k_i^j	C^k	r_i^{2l}
25	2.50	2.50	0.772	4.825	0.9889	0.56	0.056	0.908	0.080	1.185	0.705
50	6.68	6.71	0.077	8.284	0.9999	0.57	0.033	0.897	0.081	5.984	0.770
75	9.78	9.86	0.093	9.041	0.9999	1.19	0.038	0.966	0.149	8.487	0.893
100	14.04	14.16	0.056	11.22	0.9999	1.87	0.036	0.978	0.239	11.96	0.922

Note: Same notation as given in Table 1.

For the adsorption of MB onto CD, the values of k_1 were estimated as 6.60 × 10^{-2}, 4.3 × 10^{-2}, 3.90 × 10^{-2}, and 8.9 × 10^{-2} min^{-1} for initial dye concentrations of 25, 50, 75, and 100 mg L^{-1}, respectively. The values of r^2 from *log* $(q_1 - q_t)$ vs. t were between 0.744 and 0.943. The values of q_1 were 0.51, 1.59, 0.40, and 2.99 mg g^{-1} for initial dye concentrations of 25, 50, 75, and 100 mg L^{-1}, respectively. They were also not in agreement with the experimental data, q_e (see Table 4). A similar result was obtained for the adsorption of MB onto pine tree leaves for initial concentrations between 20 and 80 mg L^{-1} by Yagub et al.[19] It was expressed that the values of q_1 from the pseudo-first-order kinetic equation did not obey the experimental data, q_e, although the values of the correlation coefficients were higher than 0.99.[19]

Table 3. Kinetic parameters for MB adsorption on CD at different initial dye concentrations.

C_0^a	q_e^b	q_2^c	k_2^d	h^e	r_2^{2f}	q_1^g	k_1^h	r_1^{2i}	k_i^j	C^k	r_i^{2l}
25	3.10	3.15	0.228	2.262	0.9997	0.51	0.066	0.744	0.096	2.358	0.577
50	8.26	8.37	0.072	5.030	0.9997	1.59	0.043	0.943	0.174	6.749	0.941
75	11.17	12.04	0.257	37.31	1	0.40	0.039	0.858	0.061	10.665	0.728
100	15.78	15.95	0.082	20.96	1	2.99	0.089	0.925	0.216	14.072	0.818

Note: Same notation as given in Table 1.

2.2.2. Intraparticle diffusion kinetics of MB adsorption on CS, CW, and CD for different initial dye concentrations

The intraparticle diffusion kinetics of MB adsorption onto CS, CW, and CD were investigated for different initial dye concentrations at pH 6.33, 20 °C, and 125 rpm.

For the adsorption of MB onto CS, the rate constant of the intraparticle diffusion (k_i) calculated from the slopes of the plots of q_t vs. $t^{1/2}$ increased from 1.09 × 10^{-1} to 1.72 × 10^{-1} (mg g^{-1} $min^{-1/2}$) with an increase in the initial dye concentration from 25 to 100 mg L^{-1} (see Table 1). The values of r^2 obtained from the plots of q_t vs. $t^{1/2}$ were 0.869, 0.976, 0.931, and 0.911 for initial dye concentrations of 25, 50, 75, and 100 mg L^{-1}, respectively. On the other hand, the C values from the intercepts of the plots of q_t vs. $t^{1/2}$ were determined. The C value indicates the thickness of the boundary layer between solute and adsorbent. From Table 2, it can be seen that the values of C increased with an increase in the initial dye concentration from 25 to 100 mg L^{-1}. The values of C were determined as 1.045, 2.463, 3.304, and 4.466 for initial dye concentrations of 25, 50, 75, and 100 mg L^{-1}, respectively.

In the adsorption of MB onto CW, the value of k_i increased from 8.0 × 10^{-2} to 23.90 × 10^{-2} (mg g^{-1} $min^{-1/2}$) with an increase in the initial dye concentration from 25 to 100 mg L^{-1} (see Table 2). The values of

r^2 from the plots of q_t vs. $t^{1/2}$ were calculated as 0.705, 0.770, 0.893, and 0.922 for initial dye concentrations of 25, 50, 75, and 100 mg L^{-1}, respectively (see Table 2). The values of C increased from 1.185 to 11.960 with an increase in the initial dye concentration from 25 to 100 mg L^{-1}.

In the case of the adsorption of MB onto CD, the values *of* k_i were found to be 9.66 $\times$ 10^{-2}, 17.40 $\times$ 10^{-2}, 6.10 $\times$ 10^{-2}, and 21.60 $\times$ 10^{-2} mg g^{-1} $min^{-1/2}$ for initial dye concentrations of 25, 50, 75, and 100 mg L^{-1}, respectively (see Table 3). The values of r^2 obtained from the plots of q_t vs. $t^{1/2}$ were found to be 0.577, 0.941, 0.728, and 0.818 for initial dye concentrations of 25, 50, 75, and 100 mg L^{-1}, respectively (see Table 3). The values of C increased from 2.358 to 14.072 with an increase in the initial dye concentration from 25 to 100 mg L^{-1}. Similar results were reported for the adsorption of MB onto sugar beet pulp[20] and rejected tea.[21]

2.2.3. The pseudo-second-order kinetics of MB adsorption on CS, CW, and CD for different initial dye concentrations

Figures 1–3 illustrate the pseudo-second-order kinetics of MB adsorption onto CS, CW, and CD for different initial dye concentrations at pH 6.33, 20 °C, and 125 rpm.

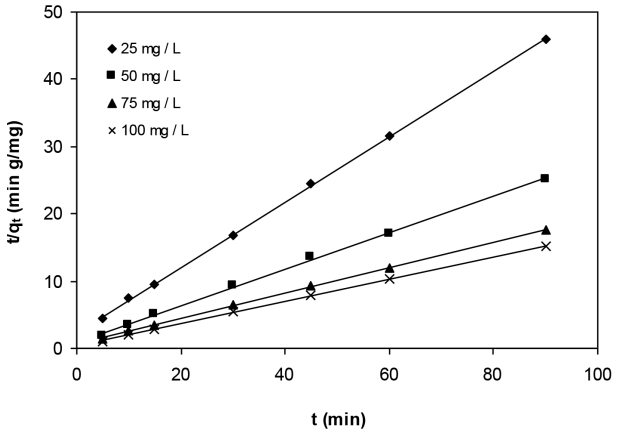

Figure 1. The pseudo-second-order adsorption kinetics of MB on CS for different initial dye concentrations (pH 6.33, 20 °C, and 125 rpm).

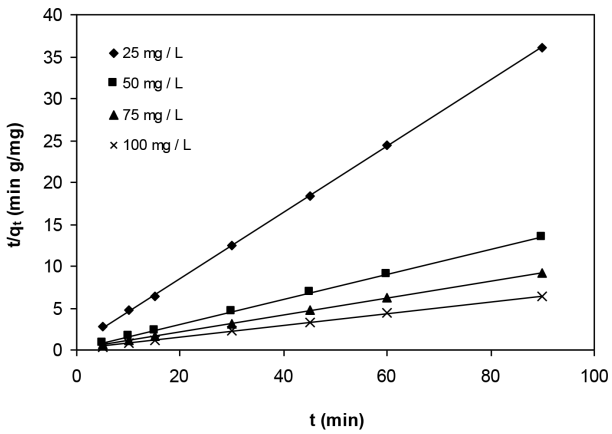

Figure 2. The pseudo-second-order adsorption kinetics of MB on CW for different initial dye concentrations (pH 6.33, 20 °C, and 125 rpm).

For the adsorption of MB onto CS, the value of the rate constants (k_2) determined from the pseudo-second-order kinetics decreased from 10.40 $\times$ 10^{-2} to 7.40 $\times$ 10^{-2} g mg^{-1} min with an increase in the initial dye concentration from 25 to 100 mg L^{-1}. The values of the initial adsorption rate, h, were 0.437, 1.122, 1.524, and 2.713 mg g^{-1} min^{-1} for initial dye concentrations of 25, 50, 75, and 100 mg L^{-1}, respectively. Similar results have been reported for both the adsorption of basic blue 69 and acid blue 25 onto peat by Ho and McKay[4] and the adsorption of malachite green onto tamarind fruit shell by Saha et al.[22] The values of r^2 obtained from the plots of the pseudo-second-order kinetics shown in Figure 1 are higher than 0.99 for all initial dye concentrations. The values of equilibrium adsorption capacity, q_2, increased from 2.05 to 6.06 mg g^{-1} with an increase in the initial dye concentration. These values of q_2 were well fitted to the experimental data, *qe*.

In the case of the adsorption of MB onto CW, the value of k_2 decreased from 7.72 $\times$ 10^{-1} to 5.60 $\times$ 10^{-2} g mg^{-1} min^{-1} with an increase in the initial dye concentration from 25 to 100 mg L^{-1}. The values

of h were 4.825, 8.284, 9.041, and 11.22 mg g^{-1} min^{-1} for concentrations of 25, 50, 75, and 100 mg L^{-1}, respectively. A similar result has also been reported for the adsorption of MB onto broad bean peels by Hameed et al.[9] The values of r^2 obtained from the plots of the pseudo-second-order kinetics illustrated in Figure 2 were higher than 0.98 for all initial dye concentrations. The value of q_2 increased from 2.50 to 14.16 mg g^{-1} with an increase in the initial dye concentration. These values of q_2 were in agreement with the experimental data, q_e.

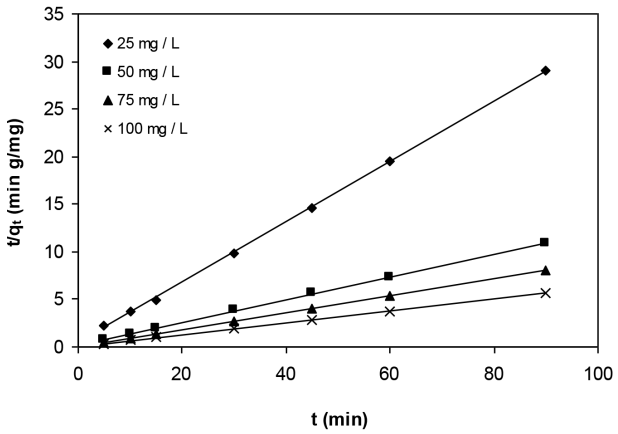

Figure 3. The pseudo-second-order adsorption kinetics of MB on CD for different initial dye concentrations (pH 6.33, 20 °C, and 125 rpm).

In the case of the adsorption of MB onto CD, the values of k_2 were determined as 22.80 × 10^{-2}, 7.20 × 10^{-2}, 25.70 × 10^{-2}, and 8.20 × 10^{-2} g mg^{-1} min^{-1} for initial dye concentrations of 25, 50, 75, and 100 mg L^{-1}, respectively. The values of h were 2.262, 5.030, 37.31, and 20.96 mg g^{-1} min^{-1} for initial dye concentrations of 25, 50, 75, and 100 mg L^{-1}, respectively. The values of r^2 from the plots of the pseudo-second-order kinetics shown in Figure 3 were between 0.999 and 1.0 for initial dye concentrations of 25, 50, 75, and 100 mg L^{-1}. The value of q_2 increased from 3.15 to 15.95 mg g^{-1} with an increase in the initial dye concentration. These values of q_2 were also in agreement with the experimental data, q_e. Similar results were recorded for the adsorption of MB onto sugar beet pulp[20] and rejected tea.[21] In a study conducted by Vucurovic et al., the pseudo-second-order kinetics was studied between the concentrations of 20 and 50 mg L^{-1} for each pH between 2 and 8 at 25 °C. It was reported that the values of r^2 obtained from the pseudo-second-order kinetics were between 0.99 and 1 under all conditions studied.[20] Nasuha et al. reported that all values of r^2 obtained from the pseudo-second-order kinetics were 0.99.[21]

2.3. Effect of pH on adsorption kinetics

The effect of initial pH on the adsorption of MB onto CS, CW, and CD was studied for the initial concentrations of 50 mg L^{-1} at 20 °C and 125 rpm as a function of contact time. The pH values of the dye solutions were selected as 5, 6.33 (natural dye pH), 8, and 10. When the pH of dye solutions was increased from 5 to 10, the equilibrium adsorption capacities increased from 2.66 to 4.52 mg g^{-1}, from 6.22 to 8.33 mg g^{-1}, and from 7.66 to 9.75 mg g^{-1} for CS, CW, and CD, respectively. For all adsorbents, the higher adsorption occurred at pH 10 and the lower adsorption occurred at pH 5. Because the surface charges of the adsorbents have become more

negatively charged at higher pH, the higher adsorption may be observed via electrostatic interactions between negatively charged adsorbents and positively charged MB molecules, a cationic dye.

2.3.1. The pseudo-first-order kinetics of MB adsorption on CS, CW, and CD for different pHs

The pseudo-first-order kinetics of MB adsorption onto CS, CW, and CD was investigated for different solution pHs at the initial dye concentration of 50 mg L^{-1} at 20 °C and 125 rpm.

For the adsorption of MB onto CS, the values of rate constants (k_1) from the pseudo-first-order model decreased with an increase in solution pH, and they were estimated to be 8.10 × 10^{-2}, 4.0 × 10^{-2}, 5.80 × 10^{-2}, and 6.90 × 10^{-2} min^{-1} for solution pHs of 5, 6.33, 8, and 10, respectively. The correlation coefficients, r^2, obtained from the plots of $log\ (q_1 - q_t)$ vs. t had values higher than 0.957. The values of equilibrium adsorption capacity (q_1) from the intercept of the plots of log $(q_1 - q_t)$ vs. t were 1.49, 1.15, 1.57, and 0.94 mg g^{-1} for solution pHs of 5, 6.33, 8, and 10, respectively. These values of q_1 were not in agreement with the experimental data, q_e (see Table 4).

Table 4. Kinetic parameters for MB adsorption on CS at different initial dye pHs.

pH[a]	q_e^b	q_2^c	k_2^d	h^e	r_2^{2f}	q_1^g	k_1^h	r_1^{2i}	k_i^j	C^k	r_i^{2l}
5	2.66	2.77	0.108	0.835	0.9998	1.49	0.081	0.991	0.126	1.645	0.845
6.33	3.59	3.68	0.083	1.122	0.9988	1.15	0.040	0.957	0.127	2.463	0.976
8	4.30	4.43	0.082	1.601	0.9999	1.57	0.058	0.995	0.165	2.935	0.881
10	4.52	4.58	0.176	3.698	1	0.94	0.069	0.974	0.109	3.658	0.725

[a]Initial dye solution pH, the other notation is the same as given in Table 1.

In the case of the adsorption of MB onto CW, the values of k_1 were calculated as 5.70 × 10^{-2}, 3.30 × 10^{-2}, 5.90 × 10^{-2}, and 7.0 × 10^{-2} min^{-1} for solution pHs of 5, 6.33, 8, and 10, respectively. The values of r^2 determined from the plots of $log\ (q_1 - q_t)$ vs. t were between 0.897 and 0.985. The values of q_1 were 1.38 and 0.57, 1.04, and 1.11 mg g^{-1} for solution pHs of 5, 6.33, 8, and 10, respectively. These values were not in agreement with the experimental data, q_e (see Table 5).

Table 5. Kinetic parameters for MB adsorption on CW at different initial dye pHs.

pH[a]	q_e^b	q_2^c	k_2^d	h^e	r_2^{2f}	q_1^g	k_1^h	r_1^{2i}	k_i^j	C^k	r_i^{2l}
5	6.22	6.40	0.066	2.715	0.9995	1.38	0.057	0.983	0.145	5.017	0.869
6.33	6.68	6.71	0.077	8.284	0.9999	0.57	0.033	0.897	0.081	5.984	0.770
8	7.81	8.01	0.067	4.292	0.9994	1.04	0.059	0.985	0.122	6.825	0.791
10	8.33	8.53	0.070	5.093	0.9994	1.11	0.070	0.975	0.113	7.425	0.760

[a]Initial dye solution pH, the other notation is the same as given in Table 1.

For the adsorption of MB onto CD, the values of k_1 were determined as 7.40 × 10^{-2}, 4.30 × 10^{-2}, 6.60 × 10^{-2}, and 7.80 × 10^{-2} min^{-1} for solution pHs of 5, 6.33, 8, and 10, respectively. The values of r^2 from the plots of $log\ (q_1 - q_t)$ vs. t were between 0.943 and 0.985. The values of q_1 were 2.77, 1.59, 0.95, and 0.69 mg g^{-1} for solution pHs of 5, 6.33, 8, and 10, respectively. These values were also not in agreement with the experimental data, q_e (see Table 6). A similar result was reported for the adsorption of MB onto sugar beet pulp.[20]

Table 6. Kinetic parameters for MB adsorption on CD at different initial dye pHs.

pH[a]	q_e^b	q_2^c	k_2^d	h[e]	r_2^{2f}	q_1^g	k_1^h	r_1^{2i}	k_i^j	C[k]	r_i^{2l}
5	7.66	7.91	0.051	3.203	0.9996	2.77	0.074	0.962	0.334	5.051	0.623
6.33	8.26	8.37	0.072	5.030	0.9987	1.59	0.043	0.943	0.174	6.749	0.941
8	9.68	9.73	0.018	1.770	1	0.95	0.066	0.985	0.094	8.917	0.836
10	9.75	9.79	0.279	26.73	1	0.69	0.078	0.968	0.078	9.130	0.723

[a]Initial dye solution pH, the other notation is the same as given in Table 1.

2.3.2. The intraparticle diffusion kinetics of MB adsorption on CS, CW, and CD for different pHs

The intraparticle diffusion kinetics of MB adsorption onto CS, CW, and CD was studied for different solution pHs at the initial dye concentration of 50 mg L^{-1} at 20 °C and 125 rpm.

For the adsorption of MB onto CS, the intraparticle diffusion rates (k_i) from the slopes of the plots of q_t vs. $t^{1/2}$ were determined as 12.60 × 10^{-2}, 12.70 × 10^{-2}, 16.50 × 10^{-2}, and 10.90 × 10^{-2} mg g^{-1} $min^{-1/2}$ for solution pHs of 5, 6.33, 8, and 10, respectively (see Table 5). The values of r^2 from the plots of q_t vs. $t^{1/2}$ were 0.845, 0.976, 0.881, and 0.725 for solution pHs of 5, 6.33, 8, and 10, respectively. The C values, indicating the thickness of the boundary layer determined from the intercepts of the plots of q_t vs. $t^{1/2}$, were 1.645, 2.463, 2.935, and 3.658 for solution pHs of 5, 6.33, 8, and 10, respectively (see Table 4).

In the case of the adsorption of MB onto CW, the value of k_i decreased from 14.50 × 10^{-2} to 11.30 × 10^{-2} mg g^{-1} $min^{-1/2}$ with an increase in the solution pH from 5 to 10 (see Table 5). The values of r^2 from the plots of q_t vs. $t^{1/2}$ were 0.869, 0.770, 0.791, and 0.760 for solution pHs of 5, 6.33, 8, and 10, respectively (see Table 5). The C values increased from 5.017 to 7.425 with an increase in the solution pH from 5 to 10.

For the adsorption of MB onto CD, the value of k_i decreased from 33.40 × 10^{-2} to 7.80 × 10^{-2} mg g^{-1} $min^{-1/2}$ with an increase in the solution pH from 5 to 10 (see Table 6). The values of r^2 from the plots of q_t vs. $t^{1/2}$ were 0.623, 0.941, 0.836, and 0.723 for solution pHs of 5, 6.33, 8, and 10, respectively (see Table 7). The values of C increased from 5.051 to 9.130 with an increase in the solution pH from 5 to 10. A similar result was reported for the adsorption of MB onto sugar beet pulp.[20] It was recorded that the value of C increased from 2.44 to 4.71 with an increase in the solution pH from 2 to 8 for the initial concentration of 50 mg L^{-1} at 25 °C.[20]

2.3.3. The pseudo-second-order kinetics of MB adsorption on CS, CW, and CD for different pHs

Figures 4–6 demonstrate the pseudo-second-order kinetics of MB adsorption onto CS, CW, and CD for different solution pHs at the initial dye concentration of 50 mg L^{-1} at 20 °C and 125 rpm.

For the adsorption of MB onto CS, the values of the rate constants estimated from the pseudo-second-order kinetics (k_2) were 10.80 × 10^{-2}, 8.30 × 10^{-2}, 8.20 × 10^{-2}, and 17.60 × 10^{-2} g mg^{-1} min^{-1} for solution pHs of 5, 6.33, 8, and 10, respectively (see Table 4). The values of the initial adsorption rate, h, were 0.835, 1.122, 1.601, and 3.698 mg g^{-1} min^{-1}, respectively. The values of r^2 from the plots of the pseudo-second-order kinetics were between 0.998 and 1 for all solution pHs. The value of equilibrium adsorption capacity, q_2, increased from 2.77 to 4.58 mg g^{-1} with an increase in the initial dye concentration. These values of q_2 were in agreement with the experimental data, q_e (see Table 4).

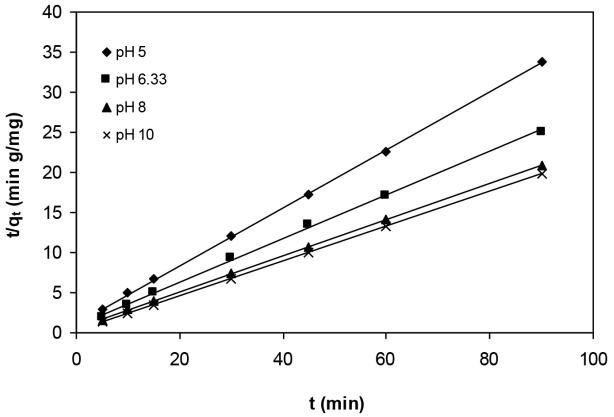

Figure 4. The pseudo-second-order adsorption kinetics of MB on CS at different solution pHs (50 mg/L, 20 °C, and 125 rpm).

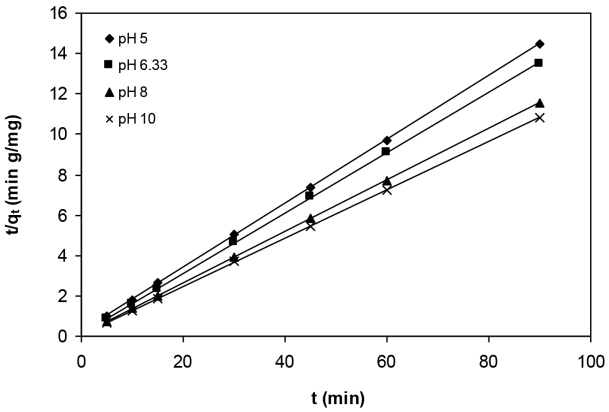

Figure 5. The pseudo-second-order adsorption kinetics of MB on CW at different solution pHs (50 mg/L, 20 °C, and 125 rpm).

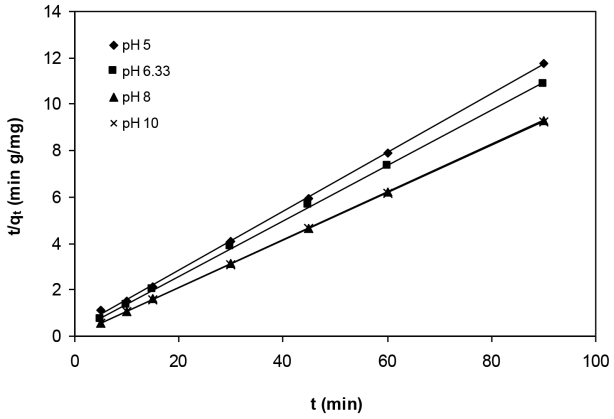

Figure 6. The pseudo-second-order adsorption kinetics of MB on CD at different solution pHs (50 mg/L, 20 °C, and 125 rpm).

In the case of the adsorption of MB onto CW, the values of k_2 were 6.60 × 10^{-2}, 7.70 × 10^{-2}, 6.70 × 10^{-2}, and 7.0 × 10^{-2} g mg^{-1} min^{-1} for solution pHs of 5, 6.33, 8, and 10, respectively (see Table 5). The values of h were 2.715, 8.284, 4.292, and 5.093 mg g^{-1} min^{-1} for solution pHs of 5, 6.33, 8, and 10, respectively. The values of r^2 obtained from the plots in Figure 5 were higher than 0.999 for all solution pHs. The value of q_2 increased from 6.40 to 8.53 mg g^{-1} with an increase in the solution pH from 5 to 10. These values of q_2 were in agreement with the experimental data, q_e (see Table 5).

For the adsorption of MB onto CD, the value of k_2 increased from 5.10 × 10^{-2} to 27.90 × 10^{-2} g mg^{-1} min with an increase in the solution pH from 5 to 10 (see Table 6). The values of h were 3.203, 5.030, 1.770, and 26.730 mg g^{-1} min^{-1} for solution pHs of 5, 6.33, 8, and 10, respectively. The values of r^2 from the plots in Figure 6 were between 0.999 and 1 for all solution pHs. The value of q_2 increased from 7.91 to 9.79 mg g^{-1} with an increase in the solution pH from 5 to 10. These values of q_2 were also in agreement with the experimental data, q_e (see Table 6). Similar results were recorded for the adsorption of MB onto sugar beet pulp between pH 2 and 8 for a constant initial dye concentration at 25 °C.[20]

2.4. Effect of temperature on adsorption kinetics

The temperature dependence of MB adsorption onto CS, CW, and CD was studied for the initial concentration of 50 mg L^{-1} at pH 6.33 and 125 rpm as a function of contact time, and the temperatures were 20, 30, 40, and 50 °C. It was observed that the adsorption slightly increased with an increase in temperature. When the temperature of dye solutions was increased from 20 to 50 °C, the equilibrium adsorption capacities increased from 3.59 to 4.40 mg g^{-1}, from 6.68 to 7.60 mg g^{-1}, and from 8.26 to 8.86 mg g^{-1} for CS, CW, and CD, respectively. The fact that the adsorption of dye onto CS, CW, and CD was slightly in favor of temperature indicates that the mobility of the dye molecule increases with a rise in temperature. Similar results have been recorded for the adsorption of MB onto perlite[12] and biosolid.[23]

2.4.1. The pseudo-first-order kinetics of MB adsorption on CS, CW, and CD for different temperatures

The pseudo-first-order kinetics of MB adsorption onto CS, CW, and CD was investigated for different temperatures at the initial dye concentration of 50 mg L^{-1} at pH 6.33 and 125 rpm.

For the adsorption of MB onto CS, the values of the rate constants (k_1) from the pseudo-first-order model increased with an increase in temperature, and they were determined as 4.0 × 10^{-2}, 7.80 × 10^{-2}, 7.20 × 10^{-2}, and 7.0 × 10^{-2} min^{-1} for temperatures of 20, 30, 40, and 50 °C, respectively. The correlation coefficients, r^2, determined from the plots of *log* $(q_1 - q_t)$ vs. t had values higher than 0.957. The values of equilibrium adsorption capacity (q_1) from the intercept of the plots of *log* $(q_1 - q_t)$ vs. t were 1.15, 1.97, 2.18, and 2.13 mg g^{-1} for temperatures of 20, 30, 40, and 50 °C, respectively. These values are not in agreement with the experimental data, q_e (see Table 7).

Table 7. Kinetic parameters for MB adsorption on CS at different initial dye temperatures.

T^a	q_e^b	q_2^c	k_2^d	h^e	r_2^{2f}	q_1^g	k_1^h	r_1^{2i}	k_i^j	C^k	r_i^{2l}
20	3.59	3.68	0.083	1.122	0.9988	1.15	0.040	0.957	0.127	2.463	0.976
30	4.03	4.17	0.085	1.472	0.9986	1.97	0.078	0.978	0.126	2.468	0.993
40	4.29	4.47	0.095	1.310	0.9993	2.18	0.072	0.974	0.185	2.763	0.908
50	4.40	4.56	0.107	1.405	0.9996	2.13	0.070	0.987	0.187	2.855	0.907

[a]The temperature of dye solution (°C), the other notation is the same as given in Table 1.

In the case of the adsorption of MB onto CW, the values of k_1 increased with an increase in temperatures, and they were found as 3.30 × 10^{-2}, 5.10 × 10^{-2}, 4.40 × 10^{-2}, and 4.0 × 10^{-2} min^{-1} for temperatures of 20, 30, 40, and 50 °C, respectively. The values of r^2 from the plots of *log* $(q_1 - q_t)$ vs. t were between 0.766 and 0.921. The values of q_1 were 0.57, 0.27, 0.21, and 0.24 mg g^{-1} for temperatures of 20, 30, 40, and 50 °C, respectively. These values were not in agreement with the experimental data, q_e (see Table 8).

Table 8. Kinetic parameters for MB adsorption on CW at different initial dye temperatures.

T^a	q_e^b	q_2^c	k_2^d	h^e	r_2^{2f}	q_1^g	k_1^h	r_1^{2i}	k_i^j	C^k	r_i^{2l}
20	6.68	6.71	0.077	8.284	0.9989	0.57	0.033	0.897	0.081	5.984	0.770
30	7.22	7.34	0.090	6.411	0.9994	0.27	0.051	0.921	0.038	6.913	0.659
40	7.50	7.63	0.106	6.170	0.9993	0.21	0.044	0.766	0.039	7.189	0.490
50	7.60	7.72	0.116	6.913	0.9994	0.24	0.040	0.821	0.026	7.365	0.924

[a]The temperature of dye solution (°C), the other notation is the same as given in Table 1.

Table 9. Kinetic parameters for MB adsorption on CD at different initial dye temperatures.

T[a]	q_e[b]	q_2[c]	k_2[d]	h[e]	r_2^2[f]	q_1[g]	k_1[h]	r_1^2[i]	k_i[j]	C[k]	r_i^2[l]
20	8.26	8.37	0.072	5.030	0.9997	1.59	0.043	0.943	0.174	6.749	0.941
30	8.56	8.67	0.122	6.178	0.9999	1.45	0.045	0.970	0.173	7.089	0.905
40	8.81	8.86	0.171	11.85	1	0.81	0.043	0.961	0.104	7.931	0.874
50	8.86	8.89	0.284	22.44	1	0.61	0.065	0.990	0.057	8.390	0.905

[a]The temperature of dye solution (°C), the other notation is the same as given in Table 1.

For the adsorption of MB onto CD, the values of k_1 were calculated as 4.30 × 10^{-2}, 4.50 × 10^{-2}, 4.30 × 10^{-2}, and 6.50 × 10^{-2} min^{-1} for temperatures of 20, 30, 40, and 50 °C, respectively. The values of r^2 obtained from the plots of *log* $(q_1 - q_t)$ vs. t were between 0.943 and 0.990. The values of q_1 were 1.59, 1.45, 0.81, and 0.61 mg g^{-1} for temperatures of 20, 30, 40, and 50 °C, respectively. These values were also not in agreement with the experimental data, q_e (see Table 9). Similar results for the pseudo-first-order kinetics were recorded for the adsorption of MB onto the waste of Abu-Tartour phosphate rock between 45 and 83 °C.[24]

2.4.2. The intraparticle diffusion kinetics of MB adsorption on CS, CW, and CD for different temperatures

The intraparticle diffusion of MB adsorption onto CS, CW, and CD was studied for different temperatures at the initial dye concentration of 50 mg L^{-1}, pH 6.33, and 125 rpm.

For the adsorption of MB onto CS, the intraparticle diffusion rates (k_i) from the slopes of the plots of q_t vs. $t^{1/2}$ were found to be 1.27 × 10^{-1}, 1.26 × 10^{-1}, 1.85 × 10^{-1}, and 1.87 × 10^{-1} mg g^{-1} $min^{-1/2}$ for temperatures of 20, 30, 40, and 50 °C, respectively (see Table 7). The values of r^2 from the plots of q_t vs. $t^{1/2}$ were 0.976, 0.993, 0.908, and 0.907 for temperatures of 20, 30, 40, and 50 °C, respectively. The C values, indicating the thickness of boundary layer from the intercepts of the plots of q_t vs. $t^{1/2}$, were 2.463, 2.468, 2.763, and 2.855 for temperatures of 20, 30, 40, and 50 °C, respectively (see Table 7).

In the case of the adsorption of MB onto CW, the value of k_i, decreased from 8.10 × 10^{-2} to 2.60 × 10^{-2} mg g^{-1} $min^{-1/2}$ with an increase in temperature from 20 to 50 °C (see Table 8). The values of r^2 obtained from the plots of q_t vs. $t^{1/2}$ were 0.770, 0.659, 0.490, and 0.924 for temperatures of 20, 30, 40, and 50 °C, respectively. The value of C, estimated from the intercepts of plots of q_t vs. $t^{1/2}$, increased from 5.984 to 7.365 with an increase in temperature from 20 to 50 °C (see Table 8).

For the adsorption of MB onto CD, the value of k_i decreased from 17.40 × 10^{-2} to 5.70 × 10^{-2} mg g^{-1} $min^{-1/2}$ with an increase in temperature from 20 to 50 °C (see Table 9). The values of r^2 obtained from the plots of q_t against $t^{1/2}$ were 0.941, 0.905, 0.874, and 0.905 for temperatures of 20, 30, 40, and 50 °C, respectively (see Table 9). The value of C increased from 6.749 to 8.390 with an increase in temperature from 20 to 50 °C. Similar results for intraparticle diffusion were also recorded for the adsorption of MB onto the waste of Abu-Tartour phosphate rock between 45 and 83 °C.[24]

2.4.3. The pseudo-second-order kinetics of MB adsorption on CS, CW, and CD for different temperatures

Figures 7–9 demonstrate the pseudo-second-order kinetics of MB adsorption onto CS, CW, and CD for different temperatures at the initial dye concentration of 50 mg L^{-1}, pH 6.33, and 125 rpm.

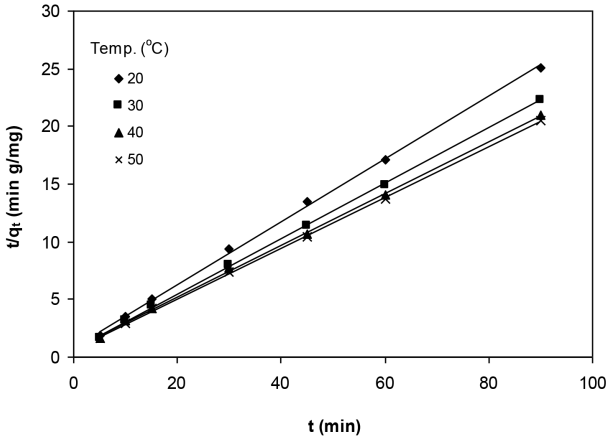

Figure 7. The pseudo-second-order adsorption kinetics of MB on CS for different temperatures (50 mg/L, pH 6.33, and 125 rpm).

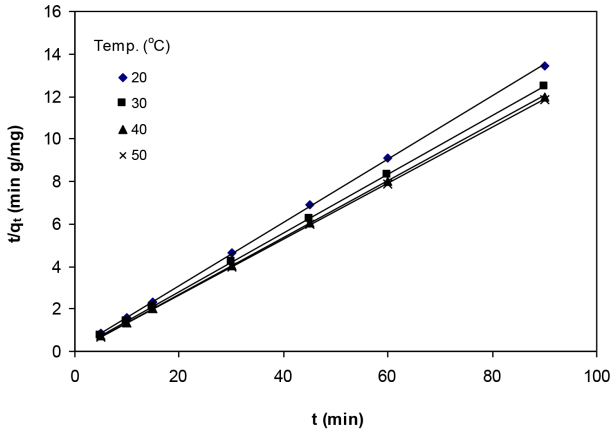

Figure 8. The pseudo-second-order adsorption kinetics of MB on CW for different temperatures (50 mg/L, pH 6.33, and 125 rpm).

For the adsorption of MB onto CS, the values of the rate constants from the pseudo-second-order kinetics (k_2) were 8.30 $\times$ 10^{-2}, 8.50 $\times$ 10^{-2}, 9.50 $\times$ 10^{-2}, and 10.70 $\times$ 10^{-2} g mg^{-1} min^{-1} for temperatures of 20, 30, 40, and 50 °C, respectively (see Table 7). The values of the initial adsorption rate, h, were 1.122, 1.472, 1.310, and 1.405, mg g^{-1} min^{-1}, respectively. The values of r^2 obtained from plots of the pseudo-second-order kinetics shown in Figure 7 were more than 0.998 for all temperatures. The value of equilibrium adsorption capacity, q_2, increased from 3.68 to 4.56 mg g^{-1} with an increase in temperature from 20 to 50 °C. These values of q_2 were in agreement with the experimental data, q_e (see Table 7).

In the case of the adsorption of MB onto CW, the values of k_2 were calculated as 7.70 $\times$ 10^{-2}, 9.0 $\times$ 10^{-2}, 10.60 $\times$ 10^{-2}, and 11.60 $\times$ 10^{-2} g mg^{-1} min^{-1} for temperatures of 20, 30, 40, and 50 °C, respectively (see Table 8). The h value decreased from 8.284 to 6.913 mg g^{-1} min^{-1} with an increase in temperature from 20 to 50 °C. The values of r^2 obtained from the plots in Figure 8 were more than 0.998 for all temperatures. The value of q_2 increased from 6.68 to 7.72 mg g^{-1} with an increase in temperature from 20 to 50 °C. These values of q_2 were in agreement with the experimental data, q_e (see Table 8).

For the adsorption of MB onto CD, the value of k_2 increased from 7.20 $\times$ 10^{-2} to 28.40 $\times$ 10^{-2} g mg^{-1} min^{-1} with an increase in temperature from 20 and 50 °C (see Table 9). The value of h increased from 5.030 to 22.44 mg g^{-1} min^{-1} with an increase in temperature from 20 to 50 °C also. The values of r^2 from the plots in Figure 9 were between 0.9997 and 1 for all temperatures. The values of q_2 varied between 8.37 and 8.89 mg g^{-1} with a change in temperature between 20 and 50 °C. These values of q_2 were also in agreement with the experimental data, q_e (see Table 9). Similar results were recorded for the adsorption of MB onto the waste of Abu-Tartour phosphate rock between 45 and 83 °C.[24]

As a result of all these findings stated above, in the case of the adsorption of MB onto CS, CW, and CD, it is clear that the values of correlation coefficients obtained from the linear plots of the pseudo-second-order equation are greater than those of the plots of the pseudo-first-order and intraparticle diffusion models under all conditions studied such as initial dye concentration, pH, and temperature, as shown in Tables 1–9. Furthermore, the values of equilibrium adsorption capacity obtained from the pseudo-second-order kinetic model, q_2, are in good agreement with the experimental data, q_e. This indicates that activated adsorption may occur between the dye molecule and the functional groups of organic components such as cellulose and lignin on CS, CW, and

CD. Similar results have also been reported for the adsorption kinetics of acid orange 10 onto organobentonite,[7] for the adsorption kinetics of direct blue and reactive blue onto lingnocellulose-based waste biopolymer,[8] and for the kinetics of MB adsorption onto perlite[12] and banana stalk waste.[25] On the other hand, if the correlation coefficients estimated from the plots of the intraparticle diffusion kinetics are more than 0.90, the regression may be regarded as linear.[25] Herein, in the case of the adsorption process with a correlation coefficient higher than 0.90 for the intraparticle diffusion kinetics of MB adsorption onto CS, CW, and CD, it may be concluded that the intraparticle diffusion rate is one of the rate limiting steps as well as the pseudo-second order kinetic model (see Tables 1–9). Similar results have been observed in a study on batch kinetic adsorption of MB onto perlite[12] and in another study on the kinetics of MB adsorption onto banana stalk waste.[25] If intraparticle diffusion is one of the rate-controlling steps, the adsorption is also governed by low activation energy. This situation is clarified by analyzing the activation energy of adsorption below.

2.5. Activation energy

The temperature of a chemical reaction generally increases the rate of the reaction. Therefore the temperature dependence results in a change in the rate constant. Herein, the activation energies of MB adsorption on CS, CW, and CD can be determined by Arrhenius' equation providing the relationship between rate constant and temperature as shown in the following:

$$k = k_0 \exp\left(\frac{-E_a}{RT}\right), \tag{4}$$

where k is the rate constant of adsorption (g mg^{-1} min^{-1}); k_0 is Arrhenius' constant, which is a temperature independent factor (g mg^{-1} min^{-1}); E_a is activation energy (kJ mol^{-1}); R is the gas constant (8.314 J mol^{-1} K^{-1}); and T is solution temperature in Kelvin (K).

In the present study, the activation energies of the adsorption process were calculated using the values of rate constants determined from the pseudo-second-order kinetic equation at different temperatures. The Arrhenius' plots drawn between $ln\ k_2$ vs. $1/T$ are demonstrated in Figure 10. The values of E_a estimated from the slopes of these plots were 7.05, 10.89, and 35.72 kJ mol^{-1} for CS, CW, and CD, respectively. These

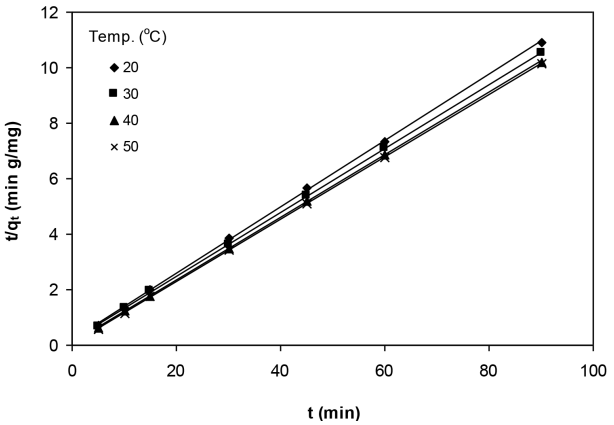

Figure 9. The pseudo-second-order adsorption kinetics of MB on CD for different temperatures (50 mg/L, pH 6.33, and 125 rpm).

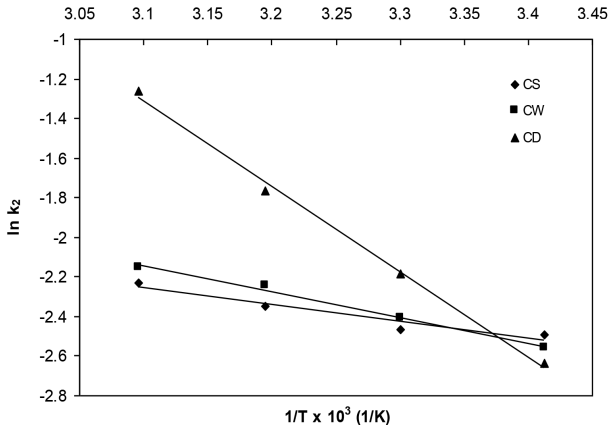

Figure 10. Arrhenius' plots for the adsorption of MB on CS, CW, and CD (50 mg/L, pH 6.33, and 125 rpm).

values of E_a are very low, and thus the adsorption of MB on these adsorbents may involve not only an activated process but also a physical adsorption process. At the same time, the small values of E_a indicate that the adsorption process may be controlled by an intraparticle diffusion mechanism. In this study, the low values of activation energies for MB adsorption on CS, CW, and CD indicate a diffusion controlled adsorption mechanism. Similar results were recorded with activation energies value of 8.50, 10.31, and 45.60 kJ mol^{-1} obtained for the adsorption of MB on pyrolyzed petrified sediment,[26] perlite,[12] and hazelnut shell,[27] respectively.

3. Experimental

3.1. Materials

3.1.1. Adsorbents

Some information about the adsorbents used in the experiments is given below.

Cotton stalk (CS), *Gossypium hirsitum* L.: Cotton stalks are the cotton plant residues after picking of cotton.

Cotton waste (CW): Cotton waste is the waste remaining after the washing of residue cotton wastes after mechanic cleaning (i.e. willow process) during the production of yarns with cotton.

Cotton dust (CD): Cotton dust is the dust of pure white cotton captured in air in the environment during the production of yarns with cotton.

In this study, CS was collected from an agricultural area in Kahramanmaraş, which is a province in southern Turkey. CW and CD samples were provided by a private spinning mill (KARSAN textile and dye factory) in Kahramanmaraş. The chemical compositions of the CS, CW, and CD were determined according to the literature,[28] and the results obtained are presented in Table 10. For the adsorption experiments, the particles that passed through 200-mesh sieves of the CS and through 20-mesh sieves of the CW and the CD were used. All of the adsorbents were utilized without any pretreatment in the experiments. However, the CS was used after drying in an oven at 105 °C for 24 h before the experiments.

Table 10. Chemical analysis of CS, CW, and CD.

	Percent values		
Component	CD	CW	CD
Cellulose	47.80	62.20	100
Holocellulose	77.50	81.70	
Lignin	21.20	14.60	
Alcohol-benzene extraction	4.70	5.60	
Ash	1.30	0.90	

3.1.2. Adsorbate

MB, a cationic dye (C. I. 52015), was purchased from Merck, and it was used as received without further purification. The stock solutions of 500–1000 mg L^{-1} were prepared with pure distilled water. pHs of the dye solutions were adjusted with diluted HCl and NaOH solutions.

3.2. Kinetic studies

For kinetic studies, adsorption experiments were carried out by shaking 0.25 g of adsorbents with aqueous solutions of 50 mL of the MB in 250-mL Erlenmeyer flasks placed in a temperature-controlled shaking water bath at different concentrations, pHs, and temperatures as a function of time. After the desired contact time,

the samples were withdrawn from the mixture by means of a micropipette, and then they were centrifuged for 5 min at 5000 rpm. After being centrifuged, supernatants were also analyzed for the determination of the final concentration of MB at a maximum absorbance wavelength of 663 nm, using a UV-Vis spectrophotometer (Jenway 6100). The amounts of MB adsorbed by adsorbents were estimated according to Eq. (5):

$$q_t = \frac{C_0 - C_t}{m} V, \tag{5}$$

where q_t is the amount of dye adsorbed (mg g^{-1}), V is the volume of the dye solution (L), m is the weight of the adsorbent (g), C_0 is the initial concentration of dye (mg L^{-1}), C_t is the amount of adsorbed at any time (mg L^{-1}), and q_t and C_t are defined as q_e and C_e in equilibrium time (mg L^{-1}).

Kinetic studies were investigated for various concentrations, pHs, and temperatures for all adsorbents (i.e. CS, CW, and CD). While the effect of any parameter such as concentration, pH, and temperature on adsorption kinetics was being investigated, the other parameters were kept constant during the experiments.

3.2.1. Concentration effect on kinetic study

The initial concentrations of MB on adsorption kinetics were selected as 25, 50, 75, and 100 mg L^{-1} at 20 °C, pH 6.33 (natural solution pH), and 125 rpm.

3.2.2. pH effect on kinetic study

The initial pHs of MB solutions on adsorption kinetics were 5, 6.33, 8, and 10 for the initial concentration of 50 mg L^{-1} at 20 °C and 125 rpm. The pHs of dye solutions were adjusted with 0.1 N HCl and NaOH solutions using a pH meter.

3.2.3. Temperature effect on kinetic study

The temperatures of MB solutions on adsorption kinetics were selected as 20, 30, 40, and 50 °C for the initial concentration of 50 mg L^{-1} at pH 6.33 and 125 rpm.

4. Conclusions

The amount of MB adsorbed on CS, CW, and CD increased with an increase in initial dye concentration, solution pH, and temperature. The equilibrium time was determined as 90 min under all experimental conditions studied such as concentration, solution pH, and temperature. The kinetics of the adsorption process was well fitted to the pseudo-second-order model. The activation energies of the adsorption were calculated using the pseudo-second-order rate constants, and they were found to be 7.05, 10.89, and 35.72 kJ mol^{-1} for CS, CW, and CD, respectively. From the values of the activation energy, it seems that the intraparticle diffusion kinetics was one of the rate-limiting steps as well as the pseudo-second order kinetics.

References

1. Ho, Y. S.; McKay, G. *Trans IChemE.* **1998**, *76(B)*, 313–318.
2. Dogan, M.; Alkan, M. *Chemosphere.* **2003**, *50*, 517–528.
3. Walker, G. M.; Hansen, L.; Hanna, J. A.; Allen, S. J. *Water Res.* **2003**, *37*, 2081–2089.
4. Ho, Y. S.; McKay, G. *Trans IChemE.* **1998**, *76(B)*, 183–191.

5. Kumar, K. V. *Process Biochem.* **2006**, *41*, 1198–1202.
6. Ahmad, R..; Kumar, R. *Clean- Soil, Air, Water* **2011**, *39*, 74– 82.
7. Jovic-Jovicic, N.; Milutinovic-Nikolic, A.; Grzetic, I.; Javonovic, D. *Chem. Eng. Technol.* **2008**, *31*, 567–574.
8. Senthilkumaar, S.; Kalaamani, P.; Subburamaan, C. V.; Subramaniam, N. G.; Kang, T. V. *Chem. Eng. Technol.* **2011**, *34*, 1459–1467.
9. Hameed, B. H.; El-Khaiary, M. I. *J. Hazard. Mater.* **2008**, *154*, 639–648.
10. Yao, Z.; Wang, L.; Qi, J. *Clean-Soil, Air, Water* **2009**, *37*, 642– 648.
11. Hameed, B. H.; Mahmoud, D. K.; Ahmad, A. L. *J. Hazard. Mater.* **2008**, *158*, 65–72.
12. Acemioğlu, B. *Chem. Eng. J.* **2005**, *106*, 73–81.
13. Ertaş, M.; Acemioğlu, B.; Alma, M. H.; Usta, M. *J. Hazard. Mater.* **2010**, *183*, 421–427
14. Lagergren, S. *Kungliga Suenska Vetens kapsakademiens. Handlingar, Band,* **1898**, *24*, 1–39.
15. Ho, Y. S.; McKay, G. *Chem. Eng. J.* **1998**, *70*, 115–124.
16. Ho, Y. S.; McKay, G. *Process Biochem.* **1999**, *34*, 451–465.
17. Weber, W. J.; Morris J. C. *J. Saint. Eng. Div. ASCE,* **1963**, *89(SA2)*, 31–59.
18. Doğar, Ç.; Gürses, A.; Açıkyıldız, M.; Özkan, E. *Colloid Surface B.* **2010**, *76*, 279–285.
19. Yakub, M. T.; Sen, T. K.; Ang, H. M. *Water Air Soil Poll.* **2012**, *223*, 5267–5282.
20. Vucurovic, V. M.; Razmovski, R. N.; Tekic, M. G. *J. Taiwan Inst. Chem. Eng.* **2012**, *43*, 108–111.
21. Nasuha, N.; Hameed, B. H.; Mohd Din, A. T. *J. Hazard. Mater.* **2010**, *175*, 126–132.
22. Saha, P.; Chowdhury, S.; Gupta, S.; Kumar, I.; Kumar, R.; *CLEAN - Soil, Air, Water* **2010**, *38*, 437–445.
23. Sarioglu, M.; Atay, U. A. *Global Nest J.* **2006**, *8*, 113–120.
24. Malash, G. F.; El-Khaiary, M. *J. Colloid Interf. Sci.* **2010**, *348*, 537–545.
25. Hameed, B. H.; Mahmoud, D. K.; Ahmad, A. L. *J. Hazard. Mater.* **2008**, *158*, 499–506.
26. Aroguz, A. Z.; Gulen, J.; Evers, R. H. *Bioresource Technol.* **2008**, *99*, 1503–1508.
27. Dogan, M.; Abak, H.; Alkan, M. *J. Hazard. Mater.* **2009**, *164*, 172–181.
28. Ertaş, M. MSc Thesis, Karadeniz Technical University, Trabzon, 2005 (in Turkish).